Front. Chem. Sci. Eng. 2020, 14(4): 513–521
https://doi.org/10.1007/s11705-019-1825-0

RESEARCH ARTICLE

Plasma-assisted oxidation of benzoic acid

Anna Khlyustova (✉), Nikolay Sirotkin

Laboratory of Chemistry of Hybrid Nanomaterials and Supermolecular Systems, G. A. Krestov Institute of Solution Chemistry of Russian Academy of Sciences, Ivanovo 153045, Russia

Abstract Plasma-assisted oxidation of organic compounds is one of the developing technologies for wastewater treatment. Plasmas effectively accelerate degradation processes due to plasma generated reactive species and ultra-violet radiation. Oxidation of BA in aqueous solutions by the atmospheric pressure glow discharge and underwater diaphragm discharge was studied and monitored by fluorescence and spectrophotometric methods. Discharge type and solution pH affect the formation rates of mono- and dihydroxybenzoic acids. Dihydroxyl derivatives were formed only by glow discharge action. The yields of hydroxyl radical were estimated on the kinetics data for the hydroxylation of benzoic acid. The steps of the hydroxylation processes and further oxidation were described.

Keywords atmospheric pressure glow discharge, underwater diaphragm discharge, oxidation, benzoic acid, hydroxyl radical

1 Introduction

Advanced oxidation processes (AOPs) such as photocatalytic oxidation, ozonation, Fenton oxidation, sonication, electrochemistry as well as non-thermal plasma treatment are being investigated as tools for organic pollutants destruction in water and wastewater [1–4]. A principal pathway of these processes is based on the interaction of highly reactive hydroxyl (OH•) radicals with organic compounds. These radicals, which are formed in aqueous solutions by thermal or photochemical reactions, are strong oxidizers (E = 2.8 V at pH < 7 and E = 1.4 V at pH > 7). Non-thermal plasma in contact or inside liquids is one of the most attractive AOPs [5]. The reactive species (hydroxyl radicals, hydrogen atoms and hydrated electrons) are formed by activation and non-equilibrium dissociation of water molecules. The previous investigations have shown that the plasma in liquids leads to the destruction of organic pollutants such as phenol [6–8] and dye compounds [9–12]. The combined technique of discharge generated in liquids with classical AOPs such as ozonation has a synergistic effect on the efficiency of treatment [13,14]. The most popular model compound is the phenol. Oxidation of phenol by different types of electrical discharges has been intensively studied, and mechanisms of destruction were described in detail [15–18]. On the other hand, the aromatic acids (terephthalic acid, benzoic acid (BA), salicylic acid, and their hydroxyl or halogen derivatives) can be also used as model pollutants.

In the present work, the BA was chosen as the model. Benzoic acid is used in textiles, plastics, chemicals, powders, catalyst, and wood bleaching, and its solution is corrosive, toxic and poisonous [19]. Because electrical discharges could induce not only destruction processes but also polymerization and synthesis of the organic compounds [20–22], we supposed that the initial processes of destruction could lead to the formation of some derivatives of the initial compound due to its reactions with reactive species. In the case of BA, its hydroxyl derivatives such as salicylic acid (2-hydroxybenzoic acid (2-HBA)) may form, and even dihydroxy- and polyhydroxy- derivatives could form by further hydroxylation processes. These compounds can register in a solution by using the fluorescence method. In the experiments with non-thermal plasma in contact or in liquid, BA and its chloro- and hydroxy-derivatives are used as chemical probes for OH radical detection [23–28]. We suppose that the main mechanism of destruction of BA is interaction with hydrogen peroxide or hydroxyl radicals as the reactants of H_2O_2. From this point of view, the two pH values were used: hydrogen peroxide is more stable in acid solutions and yield of hydroxyl radicals is higher in alkali ones.

The objective of the present study is to compare two types of electrical discharge on oxidation efficiency of BA. Direct current atmospheric pressure glow discharge

Received November 8, 2018; accepted February 18, 2019

E-mail: avlada5577@gmail.com

(APGD) and underwater alternative current (AC) diaphragm discharge (DD) were selected as two different discharge types. The APGD is one of the plasmas in contact with liquid, which is ignited above a solution surface. The chemical transformations occur at thin solution layer under the cathode spot. The underwater electrical discharge generates the non-thermal plasma in a liquid phase. The underwater AC diaphragm discharge is perspective for the applications in the technological process due to its relative simplicity. It does not need specific equipment, for example, an expensive high voltage pulsed source. In the present work, AC source operated at 50 Hz frequency with 0.8−4 kV voltage and 20−500 mA discharge current was used. The novelty of this study is to analyze the chemical pathways of oxidation processes in liquids, which occurred during the discharge treatment. In addition, we estimated yields of hydroxyl radical production.

2 Materials and methods

2.1 Materials

All reagents were used without further purification. BA, salicylic acid (2-HBA), 2,3- and 2,5-dihydroxybenzoic acids (diHBAs), pyrocatechol (Cat), hydroquinone (HQ), and *p*-benzoquinone (*p*-BQ) were purchased from Sigma-Aldrich (USA). The sodium hydroxide and nitric acid were obtained from Chimmed (Russia). All aqueous solutions were prepared in distilled water. Five mmol/L aqueous solution of BA was prepared and stored at room temperature.

The solution pH was initially adjusted to 3.5 or 10 by adding an appropriate amount of NaOH or HNO_3, respectively. In neutral solutions, the formation of non-stable hydroxycyclohexadienyl radicals occurs due to hydrated electrons and hydrogen atoms presence [29]. The solution pH was measured by pH meter (I-160MI, Russia). No change in pH was observed during the discharge treatment.

2.2 Experimental setup

All experiments were conducted in a non-symmetrical glass H-type cell in an open air at the constant volume of a solution (170 mL). The configuration of the cell was the same for both types of plasma discharge and described elsewhere [30,31]. In the experiments using glow discharge, the discharge was ignited above the liquid cathode surface at atmospheric pressure. The platinum wires were used as the electrodes. The interelectrode gap was constant (3 mm). Discharge current varied in the range from 10 to 50 mA. In this case, the configuration of the cell can prevent reduction processes caused by molecular hydrogen that formed at the metallic cathode.

In experiments using underwater AC diaphragm discharge, graphite rods with a diameter of 5 mm were used as the metallic electrodes. Two voltage probes were connected to an ADC miniLab 1008. Measurements from the probes were recorded by a PC program "TracerDAQ". The instantaneous power was calculated using Eq. (1):

$$P = \frac{1}{T}\int_0^t I(t)\cdot U(t)\mathrm{d}t, \tag{1}$$

where $I(t)$ is the discharge current (A), $U(t)$ is the applied voltage (V), T is the averaging time (it was decided to average over several periods to have a realistic estimation of the dissipated power), and t is a time of an experiment.

In the case of glow discharge, the input power is estimated as follow: $P = iU_c$, where i is a discharge current, and U_c is a cathode potential fall. To estimate the cathode potential fall, several experiments of voltage distribution in the inter-electrode gap were carried out by moving anode method [32]. The voltage of burning discharge was measured at different distances between metal anode and solution surface. The distance was changed from 0.5 to 2.5 mm by moving anode. The obtained data were fitted by a linear function, and the extrapolation to zero distance allows estimating the cathode potential fall value. The obtained results have shown that U_c values do not depend on discharge current for both media. The values are 660±20 and 580±15 V for acid and alkali solutions, respectively. Average values of power for both types of electrical discharge are depicted in Fig. 1.

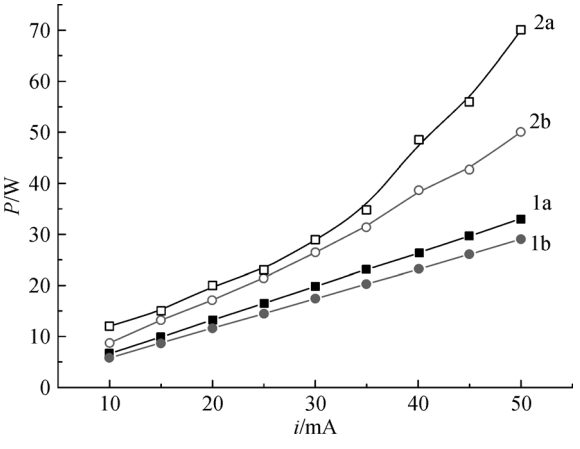

Fig. 1 Average values of input power of (1) glow discharge and (2) underwater AC diaphragm discharge at pH (a) 3.5 and (b) pH 10.

2.3 Analysis

2-HBA, 2,3- and 2,5-diHBAs were analyzed by the fluorescence method. Fluorescence spectra have been registered using spectrofluorimeter Cary Eclipse (Varian-Agilent, USA-Australia) with the xenon lamp as a pulsed

radiation source in the range of 300−600 nm. The width of the slits for excitation and emission were 5 nm in the case of 2-HBA and 10 nm in the case of 2,3- and 2,5-diHBAs. Samples (4 mL) were placed in a standard quartz cuvette with an optical length of 1 cm. 2-HBA has a bright fluorescence with emission at 420 nm and excitation of UV light at 320 nm [33–36]. 2,3- and 2,5-diHBAs are also fluorophore with emission wavelength at 407 nm and excitation of UV light at 290 nm [33]. The registration system was calibrated with solutions of 2-HBA, 2,3- and 2,5-diHBAs with known concentrations. Because fluorescence spectra of 2,3- and 2,5-diHBAs are superimposed [33], we have registered the sum intensity of 2,3-diHBA and 2,5-diHBA (denoted as ∑diHBA).

The oxidation processes were monitored by a photometric method using spectrophotometer SF 103 (Akvilon, Russia) in the wavelength range of 190−900 nm. Samples (4 mL) were collected from the treated solution and placed in a standard quartz cuvette with an optical length of 1 cm. The concentration of products of further oxidation was determined by absorption at 455 nm from calibration curves of several standard solutions of Cat, HQ, *p*-BQ and their mixture [37].

The accumulation of hydrogen peroxide was detected using the colorimetric method with titanium oxysulfate at 410 nm [38].

3 Results and discussion

3.1 Formation of mono and diHBAs

The kinetic curves of 2-HBA accumulation in solutions during glow discharge and underwater diaphragm discharge treatments are shown in Fig. 2(a). For the experiments using underwater AC diaphragm discharge, the accumulation curves have a maximum value, suggesting that 2-HBA is a transient product. After 9 min of DD treatment, the consumption rate of 2-HBA becomes larger than its formation rate. These results show that there are optimal conditions for 2-HBA formation. For the experiments with glow discharge, the alkali medium is more appropriate, whereas the acid solution is more suitable for the formation of 2-HBA in the case of DD treatment.

Rates of formation were estimated by initial parts of kinetic curves. The effect of discharge current on the rate of formation is presented in Fig. 2(b). The rates of formation of the 2-HBA are lower by underwater diaphragm discharge treatment than by glow discharge. In our previous work [31], it was found that more than 50% of input power (energy) is consumed onto solution heating, whereas 30% energy is consumed on heat content increasing (including solution heating and the Fourier heat losses) in the case of the glow discharge with liquid cathode [32]. This indicates that the thermal destruction of BA and 2-HBA may occur in the experiments with underwater diaphragm discharge, leading to the lower rates of 2-HBA formation.

It should be noted that the discharge current has a little effect on the changes in the formation rates for all hydroxylated products (as will be shown below).

The kinetics of the sum 2,3- and 2,5-diHBAs are shown in Fig. 3(a). The experimental results show that the accumulation of diHBAs was detected after the third minute of APGD treatment. It was also found experimentally that the fluorescence of diHBAs was absent when discharge current was less than 20 mA in alkali solution and less than 25 mA in the acid one. The values of ΣdiHBA rapidly become constant in both media, indicating that the formation rate is equal to the rate of consumption. The consumption can include the decomposition of diHBAs [39] as well as the formation of polyhydroxybenzoic acids.

The accumulation of sum 2,3- and 2,5-diHBAs was not observed in the experiments with underwater diaphragm discharge, but the formation rates for two pHs differ by two orders of magnitude (Fig. 3(b)).

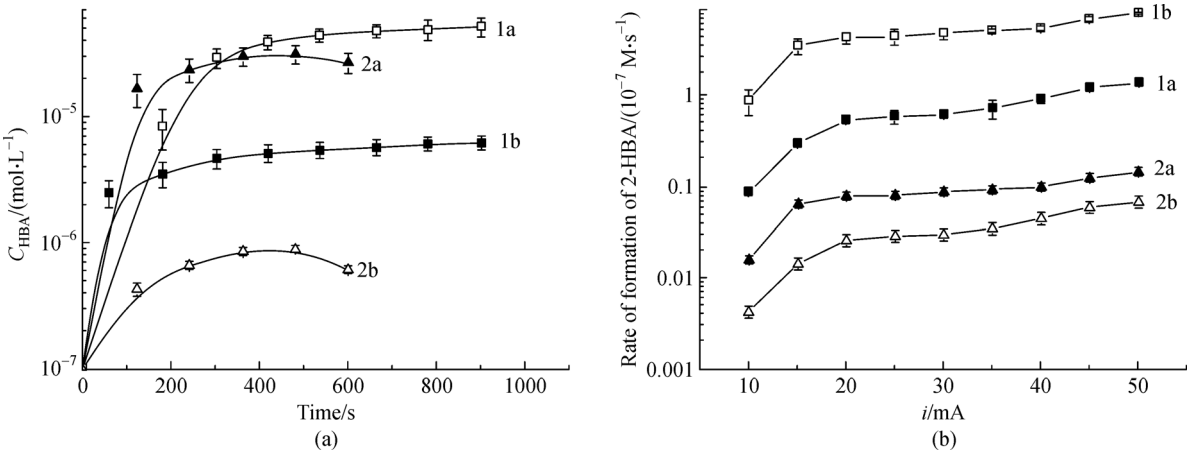

Fig. 2 (a) Accumulation kinetics and (b) rate of formation of the 2-HBA in solution by (1) glow discharge and (2) underwater diaphragm discharge at pH (a) 3.5 and (b) 10.

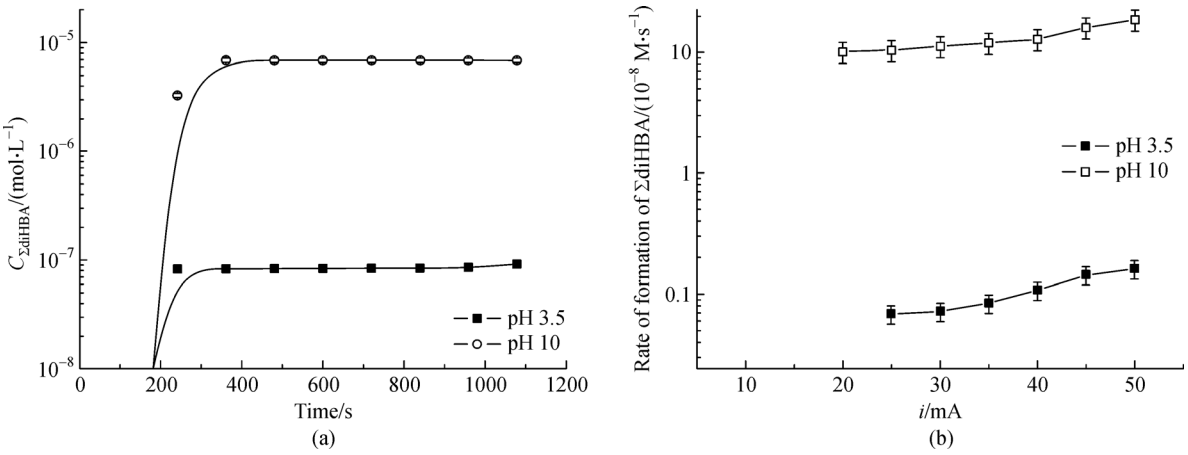

Fig. 3 Kinetic curves of (a) accumulation and (b) rate of formation of the ∑diHBA by glow discharge.

The charged particles in glow discharge lead to the formation of several radicals and reactive species like OH, H, O, O_3, etc., through collisions with water vapor molecules in the gas phase. Further, the main charged particles (mainly H_2O^+ ions) accelerated by the cathode potential fall react with water molecules in a liquid, leading to the formation of H atoms, OH radicals, and hydrated electrons. Mean free path of H_2O^+ ions in water is about 0.03 μm [40]. The diameter of the cathode spot varies from 2.5 to 3.8 mm and depends on the discharge current [41], so the active volume of solution varies from 1.38×10^{-4} to 3.54×10^{-4} μL, which is less than that reported by Lee et al. (0.21 μL) [42]. The effective lifetime of reactive species in this volume is 0.16 μs, suggesting that the diffuse length of OH radicals varies from 14 nm to 36 nm and all activation processes occur in active volume directly under the cathode spot. Maximov et al. observed that conventional flows appear from cathode spot to the bulk of solution and back, leading to a mixing of the solution [43]. We could assume that 2-HBA and diHBAs form in a small volume of the solution under the cathode spot and then travel into the bulk of a solution by convention flows.

In the case of underwater AC diaphragm discharge, the plasma is initiated and takes place in a bubble that is formed close to the diaphragm. The mechanism of bubble formation and physical processes in the underwater diaphragm discharge were described in detail in previous reports [30,44]. When a bubble is collapsed, the convention flows appear and products of plasma (reactive species) are distributed in a solution volume. Among the reactive species, the oxidative (OH• radicals) and the reductive (solvated electrons ($e_{aq}\bar{o}$), H• atoms) species are formed in a solution [30].

The first step oxidation of BA occurs via attachment of OH• radical to the aromatic ring. As a result, a HBA forms (Scheme 1). The detail processes for the formation of 2-HBA were described by Clayden et al. [45]

The second oxidation step is the further interaction of

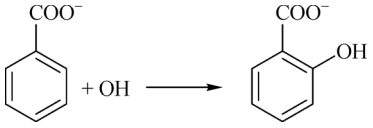

Scheme 1 Formation of 2-HBA.

OH• radicals with 2-HBA to form diHBAs in solutions as the main products (Scheme 2). Hydroxyl radicals have a strong preference to attack the *ortho*- and *para*- positions due to its electrophilic reactivity [46].

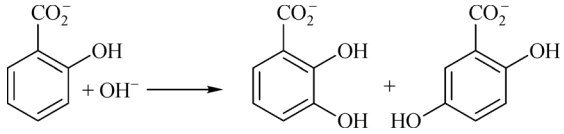

Scheme 2 Formation of 2,3- and 2,5-diHBAs.

3.2 Further destruction by electrical discharges

Continuous plasma treatment shows that the treated solutions become yellow after 11 min by APGD treatment and after 7 min by DD treatment. The absorbance spectrum has the peak at 455 nm. Figure 4 presents the time-dependence of absorbance at 455 nm. A similar solution color was detected by thermal destruction of the salicylic acid solution [37], during phenol oxidation by Fenton's reagent [47] and by discharge plasma treatment [8,48]. Bobkova et al. attributed this color to the formation of nitrophenols [8]. It was expectable because glow discharge operates in air at atmospheric pressure and nitric oxide penetrates in a liquid from the gas phase. However, these compounds have absorbance peaks at 318 and 350 nm for *ortho*- and *para*-nitrophenols, respectively [49]. The peak at 455 nm related to isomers of a benzoquinone [37,47]. In our experiments, the peaks at 318 and 350 nm did not appear.

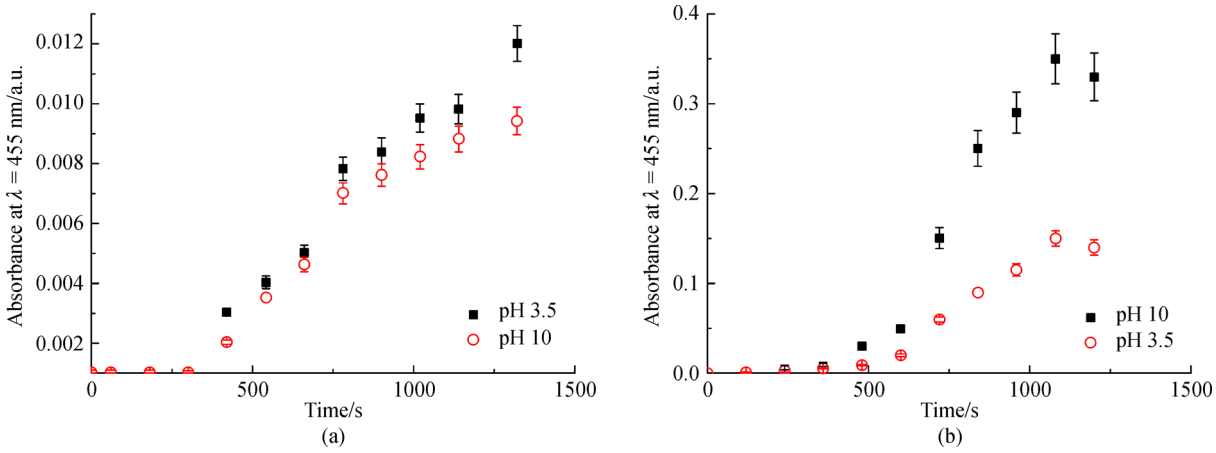

Fig. 4 Time-dependence of solution color changes (absorbance at λ = 455 nm) at two pHs by (a) glow discharge and (b) underwater diaphragm discharge.

Our experimental results show that the mixture of Cat, HQ, and *p*-BQ form during underwater diaphragm discharge whereas the *p*-BQ forms during APGD treatment only. All single solutions of these compounds have an absorbance at 455 nm, but intensity values are very low. On the other hand, the absorbance of the mixture is comparable with our experimental data. The maximum concentrations of *p*-BQ during glow discharge treatment are 5 μmol/L and 3.9 μmol/L at pH 3.5 and pH 10, respectively. In the experiments with underwater diaphragm discharge, the maximum concentrations of Cat, HQ, and *p*-BQ mixture are 63 μmol/L and 150 μmol/L at pH 3.5 and pH 10, respectively.

As shown in Fig. 5, the formation rates of quinones are comparable with the production rates of 2-HBA (Fig. 2(b)), indicating that the conversion process takes place. Because the formation of quinones was detected in all range of discharge currents, we can assume that this process may occur without the formation of diHBAs.

In the experiments with the underwater diaphragm discharge, the destruction process of 2-HBA proceeds via decarboxylation to phenol by the reductive reactive species (H• atoms in acid medium and solvated electrons ($e_{aq}\bar{o}$) in an alkali solution) (Scheme 3). Further oxidation by OH• radicals induces the formation of HQ and *p*-BQ. In the experiments with glow discharge, the oxidation process of the 2,5-diHBA proceeds via decarboxylation to HQ, which is further oxidized into colored *p*-BQ (Scheme 4). Similarly, 2,3-diHBA is oxidized through the catechol

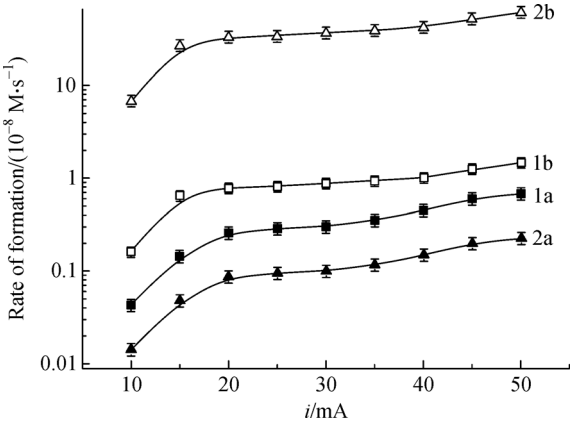

Fig. 5 Formation rates of *p*-BQ (1) by glow discharge and mixture of Cat, HQ and (2) by underwater diaphragm discharge at pH (a) 3.5 and (b) 10.

formation and transformed to *o*-benzoquinone (Scheme 5) [50].

3.3 Detection of H_2O_2

In the experiments with both types of discharge, we detected very low concentration of H_2O_2. The concentrations of H_2O_2 are 0.5 μmol/L and 0.1 μmol/L for glow discharge and diaphragm discharge, respectively. These values are very low in comparison with data for these types

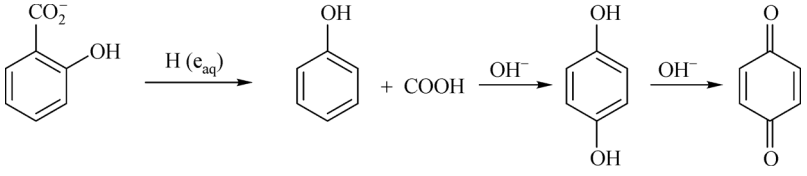

Scheme 3 Conversion of 2-HBA and formation of HQ and *p*-BQ.

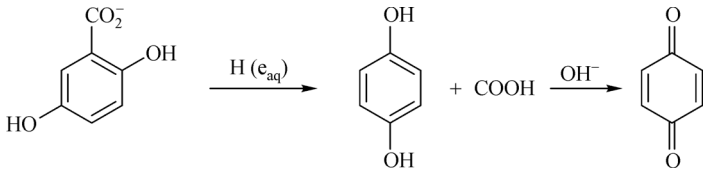

Scheme 4 Conversion of 2,5-diHBA.

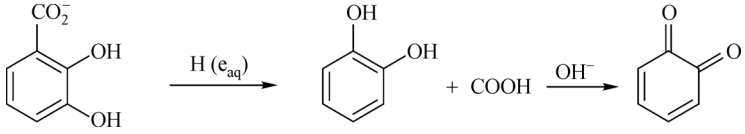

Scheme 5 Transformation of 2,3-diHBA and formation of *o*-benzoquinone.

of discharges [31,51]. We assume that the reactants for production of H_2O_2 can consume with BA and its hydroxylated derivatives. Several experiments were conducted with H_2O_2 (ratio BA/H_2O_2 was 1:1) without electrical discharge. The obtained results showed that the hydroxylation process did not occur. These data are in good agreement with the reported results that the formation of salicylic acid occurs at a high concentration of H_2O_2 or in the presence of Fe^{2+} or Cu^{2+} ions [52,53]. In our case, this means that most of the reactants for hydrogen peroxide consumed with organic substances.

3.4 Chemical pathways

Taking into consideration the reaction schemes presented above, we can propose the stepwise hydroxylation of BA by glow discharge or by underwater diaphragm discharge (Fig. 6). According to the literature [54], the yields of 3-HBA and 4-HBA are the same as that of 2-HBA. The yields for dihydroxyl derivatives can vary from 1.5% to 9.5%. Our estimations of the product yields show that the formation of *para*-benzoquinone or further hydroxylation products is likely at pH 3.5 during the glow discharge treatment. Taking into consideration the low yield of HBA in acid media, we suggest that the oxidation of 2-HBA to *p*-BQ bypasses the formation of diHBA. In the alkali solutions, however, BA is converted into *p*-BQ via the formation of mono- and di-HBA due to high yield of OH• radicals.

In the experiments with underwater diaphragm discharge, we have the opposite results. The alkali solution is more suitable media for conversion of BA into quinones.

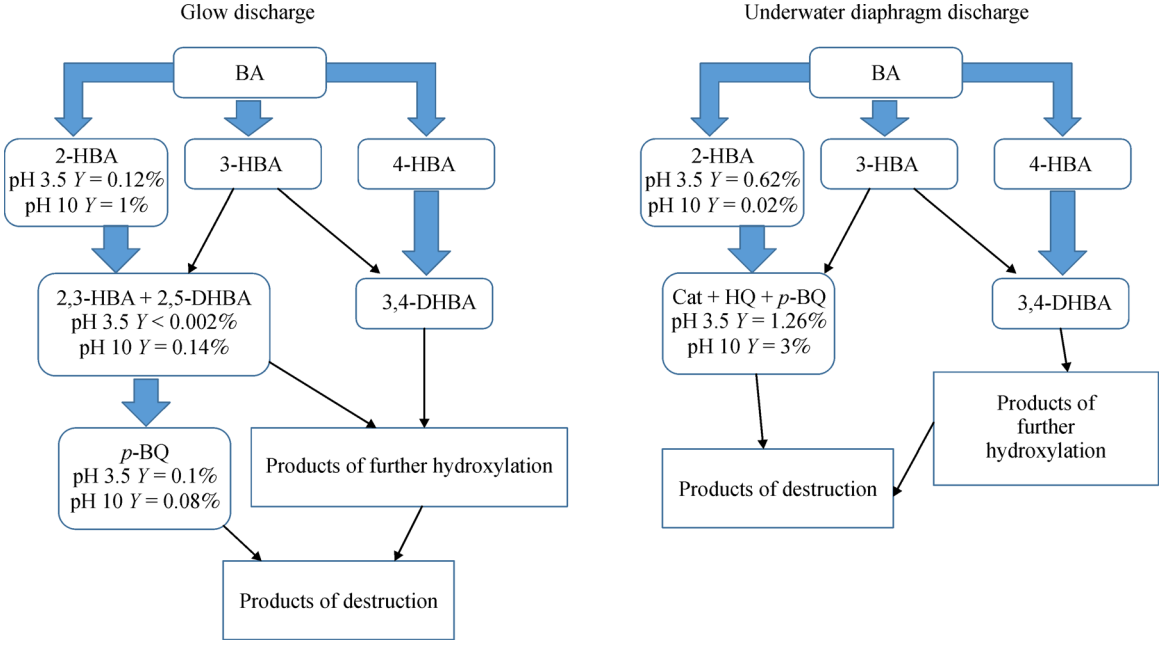

Fig. 6 The stepwise conversion of BA during glow discharge or underwater diaphragm discharge treatment.

3.5 Estimations of yields of the OH• radicals

There are several reports related to quantification of hydroxyl radicals by using benzoic and salicylic acids as the chemical probes (scavengers) [24–28,50,54,55]. For calculation of the yield of the hydroxyl radicals, we considered the assumption that the radical product yield is proportional to the fast reaction product yield at the following condition: $k[C] > 10^7$ s^{-1}, where k is rate constant and [C] is a concentration of a chemical probe. This is true in the absence of competitive reactions in solution [56]. At our experimental condition, $k_1[BA] = 4.3 \times 10^9 \times [5 \times 10^3] = 2.15 \times 10^7$ s^{-1}. Therefore, we can estimate the yield of OH radicals using the data of concentrations of 2-HBA and sum of 2,3-diHBA and 2,5-diHBA.

The kinetics of the first step of hydroxylation of BA is written as:

$$-\frac{d[BA]}{dt} = k_1[OH][BA] = v(HBA), \quad (2)$$

and the rate of second stage is:

$$\frac{d[\Sigma diHBA]}{dt} = k_2[OH][HBA] = v(\Sigma diHBA). \quad (3)$$

Then, the formation rate for hydroxyl radicals can be written as follow:

$$v(OH) = v(HBA) + v(\Sigma diHBA), \quad (4)$$

Assuming that hydroxyl radicals take part in the formation processes of *p*-BQ and HQ, the rates of its formation also include in the Eq. (4) for OH radicals.

$$v(OH) = v(HBA) + v(\Sigma diHBA) + v(p\text{-BQ})$$

$$\text{for glow discharge,} \quad (5)$$

$$v(OH) = v(HBA) + 2v(Cat + HQ + p\text{-BQ})$$

$$\text{for diaphragm discharge.} \quad (6)$$

Because the rate of formation depends on various parameters (a type of discharge, applied power, solution volume, etc.), the term "energetic yield" is acceptable for comparison with published data. It is a number of formed reactive species per input power. The energetic yield is calculated by using the following equation:

$$G = \frac{v(OH)N_A Ve}{P} \times 100 \text{ (molecules/100eV)}, \quad (7)$$

where v(OH) is production rate of OH radicals, M/s, N_A Avogadro's number (6.02×10^{23} molecule/mole), V solution volume (0.17 L), e charge of an electron (1.6×10^{-19} Coulomb), and P is the input power.

Our calculations show that G values do not depend on the discharge current in the frame of errors under our experimental conditions. But the pH of solution and type of discharge affect yield of OH radicals. Calculated yields are presented in Table 1. For alkali solutions, G values are comparable with our previous data [30,31]. In the case of acid solutions, the obtained yields are lower than those obtained early for both types of discharge. In the alkaline solutions, however, the values of energetic yields are comparable with published data [24–28].

Table 1 Effect of solution pH on energetic yields of hydroxyl radicals (molecules/100 eV)

Solution pH	Glow discharge	Underwater diaphragm discharge
3.5	$(6.0\pm0.9)\times10^{-3}$	$(8.9\pm0.2)\times10^{-3}$
10	$(6.9\pm0.4)\times10^{-2}$	$(2.3\pm0.7)\times10^{-2}$

The low energetic yields of the OH• radicals in acid media for both types of electrical discharge can connect with the difference of electrical parameters. The presence of alkaline metal facilitates the burning discharge due to less ionization potential (ionization potential for Na is 5.14 eV and for HCl is 12.54 eV). It reflects in values of discharge power (Fig. 1). On the other hand, the high yield of hydroxyl radicals in alkaline solutions can be explained by the instability of hydrogen peroxide.

4 Conclusions

In this work, oxidation of BA in aqueous solutions by two types of discharge plasma treatment has been studied. The chosen discharges, namely, the glow discharge and diaphragm discharges operated at atmospheric pressure, are often utilized for surface processing and represent high interest for several applications as the chemical processing of unwanted toxic products.

In the experiments with glow discharge, the destruction of BA includes two steps of hydroxylation and formation of the mono- and diHBAs. In the experiments with underwater diaphragm discharge, only one step of hydroxylation occurs, suggest that underwater electrical discharges could lead to the intensification of the oxidation process without the formation of the intermediates.

The formation rates of oxidation products by the glow discharge and underwater diaphragm discharge treatment were estimated. The formation rates of further oxidation products are comparable with that of the initial hydroxylation of BA. In the experiments with glow discharge, the yields of the 2-hydroxybenzoic and diHBAs are higher in alkaline solutions than in acid solutions, probably due to the higher yield of hydroxyl radicals at pH 10 than in acid solutions.

Acknowledgements This work was partially supported by RFBR (project No. 16-33-60061).

References

1. Moreira F C, Boaventura R A, Brillas E, Vilar V J. Electrochemical advanced oxidation processes: A review on their application to synthetic and real wastewaters. Applied Catalysis B: Environmental, 2017, 202: 217–261
2. Antonopoulou M, Evgenidou E, Lambropoulou D, Konstantinou I. A review on advanced oxidation processes for the removal of taste and odor compounds from aqueous media. Water Research, 2014, 53: 215–234
3. Oturan M A, Aaron J J. Advanced oxidation processes in water/wastewater treatment: Principles and applications. A review. Critical Reviews in Environmental Science and Technology, 2014, 44(23): 2577–2641
4. Chaplin B P. Critical review of electrochemical advanced oxidation processes for water treatment applications. Environmental Science. Processes & Impacts, 2014, 16(6): 1182–1203
5. Bruggeman P J, Kushner M J, Locke B R, Gardeniers J G E, Graham W G, Graves D B, Hofman-Caris R C, Maric D, Reid J P, Ceriani E, et al. Plasma-liquid interactions: A review and roadmap. Plasma Sources Science & Technology, 2016, 25(5): 053002
6. Hoeben W F L M, van Veldhuizen E M, Rutgers W R, Kroesen G M W. Gas phase corona discharges for oxidation of phenol in an aqueous solution. Journal of Physics. D, Applied Physics, 1999, 32 (24): L133–L137
7. Hoeben W F L M, van Veldhuizen E M, Rutgers W R, Cramers C A M G, Kroesen G M W. The degradation of aqueous phenol solutions by pulsed positive corona discharges. Plasma Sources Science & Technology, 2000, 9(3): 361–369
8. Bobkova E S, Sungurova A V, Rybkin V V. Mechanism of phenol degradation processes induced by direct-current atmospheric-pressure discharge in air. High Energy Chemistry, 2013, 47(4): 198–200
9. Magureanu M, Bradu C, Piroi D, Mandache N B, Parvulescu V. Pulsed corona discharge for degradation of methylene blue in water. Plasma Chemistry and Plasma Processing, 2013, 33(1): 51–64
10. Jiang B, Zheng J, Qiu S, Wu M, Zhang Q, Yan Z, Xue Q. Review on electrical discharge plasma technology for wastewater remediation. Chemical Engineering Journal, 2014, 236: 348–368
11. García M C, Mora M, Esquivel D, Foster J E, Rodero A, Jimenez-Sanchidrian C, Romero-Salguero F J. Microwave atmospheric pressure plasma jets for wastewater treatment: Degradation of methylene blue as a model dye. Chemosphere, 2017, 180: 239–246
12. Bansode A S, More S E, Siddiqui E A, Satpute S, Ahmad A, Bhoraskar S V, Mathe V L. Effective degradation of organic water pollutants by atmospheric non-thermal plasma torch and analysis of degradation process. Chemosphere, 2017, 167: 396–405
13. Khlyustova A V, Maksimov A I, Panova D S. Effect of electric discharges and oxidizing agents on aqueous solutions of a mixture of two organic dyes. Surface Engineering and Applied Electrochemistry, 2013, 49(4): 272–277
14. Khlyustova A V, Maksimov A I. Plasma-assisted oxidative degradation of organic dyes in solution by the joint action of underwater discharge and ozone. High Energy Chemistry, 2013, 47 (3): 140–143
15. Joshi A A, Locke B R, Arce P, Finney W C. Formation of hydroxyl radicals, hydrogen peroxide and aqueous electrons by pulsed streamer corona discharge in aqueous solution. Journal of Hazardous Materials, 1995, 41(1): 3–30
16. Lukes P, Locke B R. Degradation of substituted phenols in a hybrid gas-liquid electrical discharge reactor. Industrial & Engineering Chemistry Research, 2005, 44(9): 2921–2930
17. Zhang J F, Chen J R, Li X Y. Remove of phenolic compounds in water by low-temperature plasma: A review of current research. Journal of Water Resource and Protection, 2009, 1(2): 99–109
18. Marotta E, Schiorlin M, Ren X, Rea M, Paradisi C. Advanced oxidation process for degradation of aqueous phenol in a dielectric barrier discharge reactor. Plasma Processes and Polymers, 2011, 8 (9): 867–875
19. Naddeo V, Landi M, Belgiorno V, Napoli R M A. Wastewater disinfection by combination of ultrasound and ultraviolet irradiation. Journal of Hazardous Materials, 2009, 168(2-3): 925–929
20. Denaro A R, Hough K O. Polymerization by glow discharge electrolysis. Electrochimica Acta, 1973, 18(11): 863–868
21. Harada K, Iwasaki T. Syntheses of amino acids from aliphatic carboxylic acid by glow discharge electrolysis. Nature, 1974, 250 (5465): 426–428
22. Munegumi T. Chemical evolution of simple amino acids to asparagine under discharge onto the primitive hydrosphere: Simulation experiments using contact glow discharge. Bulletin of the Chemical Society of Japan, 2014, 87(11): 1208–1215
23. Gupta S B, Bluhm H. Pulsed underwater corona discharges as a source of strong oxidants: OH• and H_2O_2. Water Science and Technology, 2007, 55(12): 7–12
24. Bian W, Zhou M, Lei L. Formation of active species and by-products in water by pulsed-high voltage discharge. Plasma Chemistry and Plasma Processing, 2007, 27(3): 337–348
25. Guo Y, Liao X, Ye D. Detection of hydroxyl radical in plasma reaction on toluene removal. Journal of Environmental Sciences, 2008, 20(12): 1429–1432
26. Liao X B, Guo Y F, He J H, Ou W J, Ye D Q. Hydroxyl radicals formation in dielectric barrier discharge during decomposition of toluene. Plasma Chemistry and Plasma Processing, 2010, 30(6): 841–853
27. Li S, Hu S, Zhang H. Formation of hydroxyl radicals and hydrogen peroxide by a novel nanosecond pulsed plasma power in water. IEEE Transactions on Plasma Science, 2012, 40(1): 63–67
28. Tang S, Lu N, Shang K, Li J, Wu Y. Detection of hydroxyl radicals during regeneration of granular activated carbon in dielectric barrier discharge plasma system. Journal of Physics: Conference Series, 2013, 418: 012104
29. Albarran G, Schuler R H. Concerted effects in the reaction of OH radicals with aromatics: Radiolytic oxidation of salicylic acid. Radiation Physics and Chemistry, 2003, 67(3-4): 279–285
30. Khlyustova A, Khomyakova N, Sirotkin N, Marfin Y. The effect of pH on OH radical generation in aqueous solutions by atmospheric pressure glow discharge. Plasma Chemistry and Plasma Processing, 2016, 36(5): 1229–1238
31. Khlyustova A, Sirotkin N, Evdokimova O, Prysiazhnyi V, Titov V. Efficacy of underwater AC diaphragm discharge in generation of

reactive species in aqueous solutions. Journal of Electrostatics, 2018, 96: 76–84
32. Sirotkin N A, Titov V A. Experimental study of heating of a liquid cathode and transfer of its components into the gas phase under the action of a DC discharge. Plasma Physics Reports, 2018, 44(4): 462–467
33. Armstrong W, Black B A, Grant D W. The radiolysis of aqueous calcium benzoate and benzoic acid solutions. Journal of Physical Chemistry, 1960, 64(10): 1415–1419
34. Armstrong W, Grant D W. The aqueous benzoate system as a sensitive dosimeter for ionizing radiations. Canadian Journal of Chemistry, 1960, 38(6): 845–850
35. Downes A M. The radiation chemistry of aqueous solutions of benzoic and salicylic acids. Australian Journal of Chemistry, 1958, 11(2): 154–167
36. Loebl H, Stein G, Weiss J. Chemical action of ionizing radiations of aqueous solutions. Part VIII. Hydroxylation of benzoic acid by free radicals produced by X-rays. Journal of the Chemical Society, 1951: 405–407
37. Collado S, Garrido L, Laca A, Diaz M. Wet oxidation of salicylic acid solutions. Environmental Science & Technology, 2010, 44(22): 8629–8635
38. Eisenberg G. Colorimetric determination of hydrogen peroxide. Industrial & Engineering Chemistry. Analytical Edition, 1943, 15 (5): 327–328
39. Guinea E, Arias C, Cabot P L, Garrido J A, Rodriguez R M, Centellas F, Brillas E. Mineralization of salicylic acid in acidic aqueous medium by electrochemical advanced oxidation processes using platinum and boron-doped diamond as anode and cathodically generated hydrogen peroxide. Water Research, 2008, 42(1-2): 499–511
40. Henley E J, Johnson E R. The Chemistry and Physics of High Energy Reactions. Washington: Washington Press, 1969, 223–226
41. Khlyustova A V, Maksimov A I. Double electrical layer at the plasma-solution interface. Contributions to Plasma Physics, 2013, 53(6): 481–491
42. Lee C, Lee Y, Yoon J. Oxidative degradation of dimethylsulfoxide by locally concentrated hydroxyl radicals in streamer corona discharge processes. Chemosphere, 2006, 65(7): 1163–1170
43. Maximov A I, Kuz'micheva L A, Khlustova A V, Titova V, Dydykin M G. Transfer of solution components to a plasma zone in chemical reactions initiated by a glow discharge in electrolyte solutions. Mendeleev Communications, 2007, 17(5): 294–295
44. Maksimov A I, Khlustova A V. Low-voltage underwater electric discharges: Physical properties and application possibilities. Plasma Physics Reports, 2013, 39(13): 1099–1103
45. Clayden J, Greeves N, Warren S. Organic Chemistry. 2nd ed. New York: Oxford University Press Inc., 2012, 471–527
46. Augood D R, Hey D H, Nechvatal A, Williams G H. Homolytic aromatic substitution. Nature, 1951, 167(4253): 725–725
47. Mijangos F, Varona F, Villota N. Changes in solution color during phenol oxidation by Fenton reagent. Environmental Science & Technology, 2006, 40(17): 5538–5543
48. Tomizawa S, Tezuka M. Kinetics and mechanism of the organic degradation in aqueous solution irradiated with gaseous plasma. Plasma Chemistry and Plasma Processing, 2007, 27(4): 486–495
49. Rabbani F, Abdollahi H, Hormozi-Nazhad M R. A second-order advantage achieved with the aid of gold nanoparticle catalytic activity. Determination of nitrophenols isomers in binary mixtures. RSC Analytical Methods, 2014, 6(9): 3056–3064
50. Gazi S, Ananthakrishnan R. Semi-quantitative determination of hydroxyl radicals by benzoic acid hydroxylation: An analytical methodology for photo-Fenton system. Current Analytical Chemistry, 2012, 8(1): 143–149
51. Kuz'micheva L A, Titova V, Maximov A I. Generation of chemically active oxidative particles in electrolyte solutions under the action of glow and diaphragm discharges. Surface Engineering and Applied Electrochemistry, 2007, 43(2): 90–93
52. Ogata Y, Tomizawa K, Yamashita Y. Photoinduced oxidation of benzoic acid with aqueous hydrogen peroxide. Journal of the Chemical Society, Perkin Transactions, 1980, 2(4): 616–619
53. Mantzavinos D. Removal of benzoic acid derivatives from aqueous effluents by the catalytic decomposition of hydrogen peroxide. Process Safety and Environmental Protection, 2003, 81 (2): 99–106
54. Oturan M A, Pinson J. Hydroxylation by electrochemical generated OH radicals. Mono- and polyhydroxylation of benzoic acid: Products and isomers distributions. Journal of Physical Chemistry, 1995, 99(38): 13948–13954
55. Jen J F, Leu M F, Yang T C. Determination of hydroxyl radicals in an advanced oxidation processes with salicylic acid trapping and liquid chromatography. Journal of Chromatography A, 1998, 796 (2): 283–288
56. Hayon E. Solute scavenging effects in regions of high radical concentration produced in radiation chemistry. Transactions of the Faraday Society, 1965, 61: 723–733